

A dinuclear extension to constrained heteroleptic Cu(I) systems†

Belén Gil, Gareth A. Cooke, Deanne Nolan, Gearóid M. Ó Máille, Sunil Varughese, Longsheng Wang and Sylvia M. Draper*

Received 18th February 2011, Accepted 13th May 2011

DOI: 10.1039/c1dt10275c

This article reports the synthesis and optical properties of three dinuclear, cationic copper complexes $[\text{Cu}_2(\mu\text{-dppm})_2(\mu\text{-L})(\text{NO}_3)_2]$ (dppm diphenyldiphosphinomethane, L: L_A 3,6-bis(2-pyridyl)-4,5-diphenyl-pyridazine, L_B 3,6-bis(2-pyridyl)-4,5-di(4-pyridyl)-pyridazine and L_C 3,6-bis(2-pyridyl)-8,9-diazafuranthene). These were formed on the reaction of $[\text{Cu}(\mu\text{-dppm})(\text{NO}_3)_2]$ with a series of N-donor (bppn) ligands L. The single crystal X-ray structures of $[\text{Cu}_2(\mu\text{-dppm})_2(\mu\text{-L})(\text{NO}_3)_2 \cdot \text{CH}_2\text{Cl}_2]$ were determined and revealed that in both, the two copper atoms are held by three bridging ligands, two dppm ligands and one bppn ligand acting as a tetradentate bridge. The absorption spectra of the complexes present a MLCT $[\text{Cu} \rightarrow \pi^*(\text{N}^{\wedge}\text{N})]$ band in the λ 370–425 nm region. These new complexes exhibit red-orange MLCT-based emission in the solid-state with lifetimes in the microsecond range. In oxygen-free dichloromethane solution, the complex $[\text{Cu}_2(\mu\text{-dppm})_2(\mu\text{-L}_C)]^{2+}$ has a long lifetime of 22.8 μs . The long emission lifetimes are attributed to a rigid conformation that precludes the possible distortion of the copper in the excited state.

Introduction

Although few in number, recent publications have begun to expose the potential of Cu(I) complexes as an alternative to Ru(II) in low-cost solar-conversion devices.^{1–3} The rich photochemistry of Ru(II),⁴ Pt(II),⁵ and Ir(III)⁶ complexes is undermined by the reliance on expensive, rare metals, which in some cases exhibit an undesirable level of toxicity. The ease of preparation of Cu(I) complexes, their ability to absorb light in the visible region, intense luminescence and low cost has captured the interest of researchers in the field. Cu(I), however, undergoes a conformational change on oxidation to Cu(II), thus decreasing device efficiencies. Strategies to overcome the resultant low quantum yields and short luminescence lifetimes of $[\text{Cu}(\text{N}^{\wedge}\text{N})_2]^+$ complexes require further development.^{1,3}

The electronic nature, bulk and rigidity of the diimine ligand all play an important role in determining the photophysical properties of Cu(I) complexes.³ Traditionally bipyridyl or phenanthroline-based systems have been used but there is scope to rethink and redesign ligand systems. A synthetic protocol which can be extended to multiple systems is very attractive and new aromatic

ligands generated by Diels–Alder cycloaddition have come to the fore in Ru(II) chemistry.^{7–10}

One development in copper chemistry has been the inclusion of stabilizing phosphine ligands, offering a significant improvement on the photophysical properties. McMillin and co-workers have demonstrated that bulky bidentate phosphines (such as POP = bis[2-(biphenylphosphino)phenyl]ether) inhibit the formation of quenching exciplexes, providing unusually long emission lifetimes and rather good quantum yields, typically in the green spectral window.^{11,12}

Another possibility is to increase the number of metal centers or to seek cooperative interactions between metal centers in a diimine-based system.¹³ Only a few examples of binuclear systems exist and these use ligands such as bipyrimidine^{14,15} or 2,5-bis(2-pyridyl)pyrazine.¹⁶ One downside is that the overall rigidity is reduced, e.g. in a transoid disposition. Rigid systems are needed to prevent distortion and/or exciplet-quenching of the excited state and thus enhance the optical properties. 2,5-Bis(2-pyridyl)tetrazines, can favour cisoid conformation and as precursors *via* inverse electron demand Diels–Alder to pyridazines offer a synthetic procedure for the inclusion of new chromophores.^{17,18}

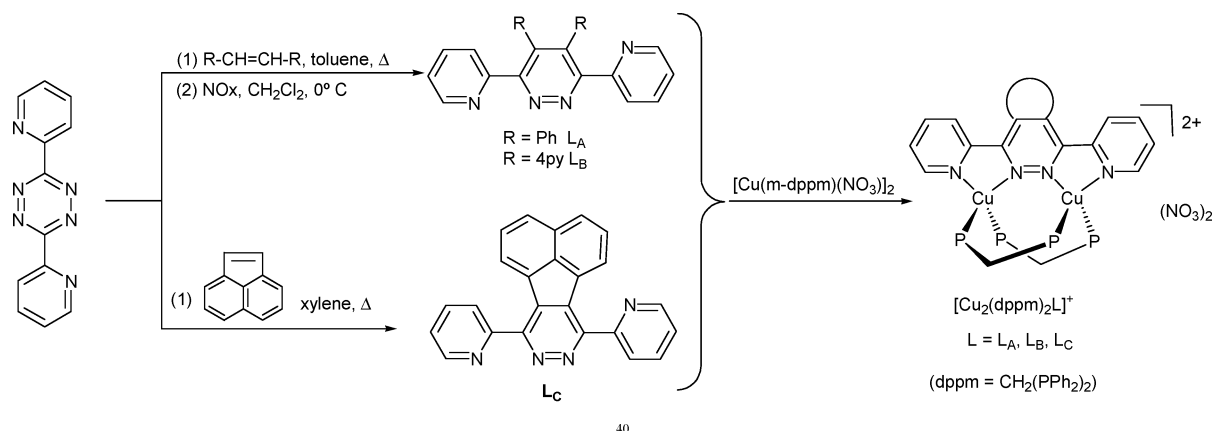
Results and discussion

Synthesis

Trans-stilbene and 1,4-bis(4-pyridyl)ethylene were each reacted with 3,4-bis(2-pyridyl)-1,2,4,5-tetrazine (*bptz*) in toluene by heating to reflux overnight in a sealed tube. On the loss of the characteristic pink colour of *bptz*, the products were

School of Chemistry, Trinity College Dublin, Dublin, 2, Ireland. E-mail: smdraper@tcd.ie; Fax: +353 1 671 2826; Tel: +353 1 896 2026

† Electronic supplementary information (ESI) available: Further crystal structures of $[\text{Cu}(\mu\text{-dppm})_2\text{L}_B]^{2+}$ and $[\text{Cu}(\mu\text{-dppm})_2\text{L}_A]^{2+}$ (Fig. S1, S2), ¹H NMR spectrum (Fig. S3) and ¹H–¹H correlation NMR spectrum (Fig. S4) of $[\text{Cu}(\mu\text{-dppm})_2\text{L}_C]^{2+}$, cyclic voltammogram of $[\text{Cu}(\mu\text{-dppm})_2\text{L}_A]^{2+}$ (Fig. S5), Comparative photophysical data of the ligands *bppn* L (Table S1). CCDC reference numbers 768169, 768170 and 824325. For ESI and crystallographic data in CIF or other electronic format see DOI: 10.1039/c1dt10275c



Scheme 1 Synthetic route towards $[\text{Cu}_2(\mu\text{-dppm})_2(\mu\text{-L})](\text{NO}_3)_2$.

purified by column chromatography to give good yields of the respective bright yellow hydropyridazines (3,6-bis(2-pyridyl)-4,5-diphenyl-hydropyridazine, 75%; 3,6-bis(2-pyridyl)-4,5-bis(4-pyridyl)-hydropyridazine, 92%). Oxidation by blowing nitrous gases¹⁹ through a dichloromethane solution of the compounds at 0 °C gave the bispyridylpyridazine (*bppn*) ligands (**L_A** 74%, **L_B** 50%, see Scheme 1). The lower yield observed for **L_B** may be due to the more electron-withdrawing 4-pyridyl substituents on the hydropyridazine ring rendering oxidation more difficult. The synthesis of **L_C** has been reported²⁰ as has the synthesis of ligand **L_A**, *albeit* under different conditions.²¹

Treatment of a colourless solution of $[\text{Cu}(\mu\text{-dppm})(\text{NO}_3\cdot\kappa^2\text{O})_2]$ in dichloromethane at room temperature with an equivalent amount of *bppn* (**L** = **L_A**, **L_B**, **L_C**) affords orange solutions. After stirring for 1 h, the resulting mixtures were filtered through Celite and concentrated (~2 mL). The addition of Et_2O (~20 mL) precipitates $[\text{Cu}_2(\mu\text{-dppm})_2(\mu\text{-L})](\text{NO}_3)_2$ as an orange solid (81%–97%). Using a 1 : 2 molar ratio of metal precursor to **L** results in the same products and unreacted **L**.

Characterisation

All the complexes are air stable as solids and in solution and were fully spectroscopically characterised (¹H and ¹³C{¹H} NMR and mass spectra) and their purity verified by elemental analysis. In addition, the structures of complexes $[\text{Cu}_2(\mu\text{-dppm})_2(\mu\text{-L})](\text{NO}_3)_2$ (**L** = **L_A**, **L_B**) were determined by single crystal X-ray diffraction. ‡

‡ **Crystallographic data.** Single crystals were carefully chosen after they were viewed through a microscope supported by a rotatable polarizing stage. The crystals were glued to a thin glass fibre using NIH immersion oil and mounted on a diffractometer equipped with an APEX CCD area detector. The data were collected either at room temperature or at 173 K. The intensity data were processed using Bruker's suite of data processing programs (SAINT), and absorption corrections were applied using SADABS. The structure solution of all the complexes was carried out by direct methods, and refinements were performed by full-matrix least-squares on F^2 using the SHELXTL-PLUS suite of programs. All the non-hydrogen atoms were refined anisotropically, and the hydrogen atoms were fixed using respective HFIX options and were refined isotropically. The solvent molecules present were highly disordered and were difficult to model. The corresponding electron density was removed from the reflection data and was refined using the SQUEEZE option in PLATON and the corresponding sqf file has been appended to the CIF. Intermolecular interactions were computed using the PLATON program. Crystallographic data for $[\text{Cu}_2(\text{dppm})_2(\text{L}_A)](\text{NO}_3)_2\cdot\text{CH}_2\text{Cl}_2$ and

Table 1 Selected bond lengths [Å] and angles [°] for $[\text{Cu}_2(\mu\text{-dppm})_2(\mu\text{-L})](\text{NO}_3)_2\cdot(\text{CH}_2\text{Cl}_2)$ (**L** = **L_A**, **L_B**)

	$[\text{Cu}_2(\mu\text{-dppm})_2(\text{L}_A)]^{2+}$	$[\text{Cu}_2(\mu\text{-dppm})_2(\text{L}_B)]^{2+}$
Cu–N _{pz}	2.014(6), 2.079(6)	2.040(3), 2.077(4)
Cu–N _{py}	2.122(7), 2.124(7)	2.150(3), 2.114(4)
Cu–P	2.232(2)–2.266(3)	2.228(1)–2.270(1)
P–Cu–P	124.65(9), 130.44(9)	124.21(5), 130.57(5)
N–Cu–N	76.3(3), 77.7(3)	76.0(1), 76.9(1)
P–Cu–N	105.8(2)–118.6(1)	104.96(9)–118.70(9)
(NCuN)–(PCuP)	87.72, 89.40	88.36, 89.24

Suitable, orange, block-shaped crystals were obtained by slow diffusion of hexane into a dry, dichloromethane solution of the respective complexes. $[\text{Cu}_2(\mu\text{-dppm})_2(\mu\text{-L})](\text{NO}_3)_2$ (**L** = **L_A**, **L_B**) crystallize in the space groups $P2_1/n$ and $P2_1/c$, respectively. For both complexes, one cation and two nitrate anions are found in the asymmetric unit together with one molecule of dichloromethane. The structures of the cations are shown in Fig. 1 for $[\text{Cu}_2(\mu\text{-dppm})_2(\mu\text{-L}_A)]^+$ and Fig. S1 for $[\text{Cu}_2(\mu\text{-dppm})_2(\mu\text{-L}_B)]^+$. † Selected bonds and angles are presented in Table 1. The anions and solvent molecules do not take part in any significant intermolecular interactions in the crystal packing.

In each case, the two copper atoms are held in close proximity by three bridging ligands: two *dppm* bonded through phosphorus and one *bppn* **L** molecule. The Cu–Cu separation ($[\text{Cu}_2(\mu\text{-dppm})_2(\mu\text{-L})](\text{NO}_3)_2$ **L_A** 3.406 Å, **L_B** 3.390 Å) is significantly longer than the sum of the van der Waals radii indicating the absence of a Cu–Cu interaction.²² Looking through the Cu...Cu axis, the conformations of the two PCuCuP bridges in each complex are approximately “eclipsed” (PCuCuP torsion

$[\text{Cu}_2(\text{dppm})_2(\text{L}_B)](\text{NO}_3)_2\cdot\text{CH}_2\text{Cl}_2$ have been deposited at the Cambridge Crystallographic Data Centre, CCDC numbers 768169 and 768170. **Crystal data for $[\text{Cu}_2(\mu\text{-dppm})_2(\mu\text{-L}_A)](\text{NO}_3)_2\cdot\text{CH}_2\text{Cl}_2$** $\text{C}_{77}\text{H}_{64}\text{Cl}_2\text{Cu}_2\text{N}_6\text{O}_6\text{P}_4$, $M_r = 1491.20$, monoclinic, $a = 14.673(3)$, $b = 19.071(4)$, $c = 26.536(6)$ Å, $\beta = 96.795(4)^\circ$, $U = 7374(3)$ Å³, $T = 301(2)$ K, space group $P2_1/n$, $Z = 4$, 40 382 reflections measured, 12 885 unique ($R_{\text{int}} = 0.1040$), which were used in all calculations. The final R_1 (all data) was 0.1471 and $wR(F_2)$ (all data) was 0.2649. **Crystal data for $[\text{Cu}_2(\mu\text{-dppm})_2(\mu\text{-L}_B)](\text{NO}_3)_2\cdot\text{CH}_2\text{Cl}_2$** $\text{C}_{75}\text{H}_{62}\text{Cl}_2\text{Cu}_2\text{N}_8\text{O}_6\text{P}_4$, $M_r = 1493.19$, monoclinic, $a = 14.570(4)$, $b = 19.092(5)$, $c = 26.482(8)$ Å, $\beta = 96.897(7)^\circ$, $U = 7313(4)$ Å³, $T = 298(2)$ K, space group $P2_1/c$, $Z = 4$, 62 142 reflections measured, 10 613 unique ($R_{\text{int}} = 0.1526$) which were used in all calculations. The final R_1 (all data) was 0.0781 and $wR(F_2)$ (all data) was 0.1283.

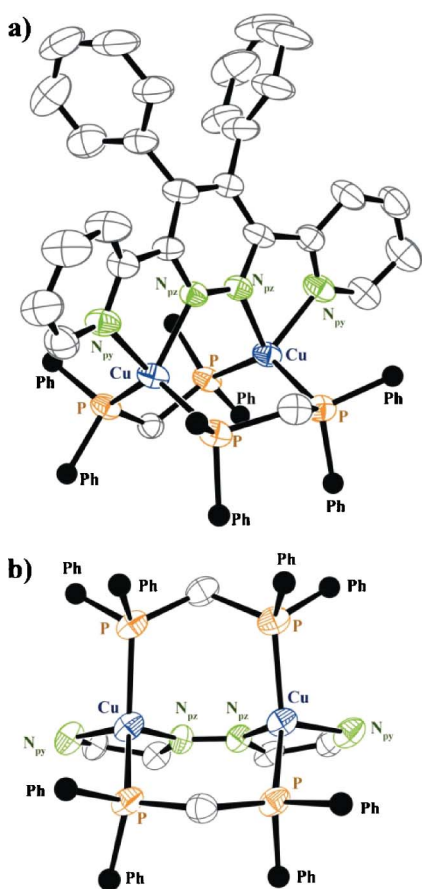


Fig. 1 (a) View of the structure of $[\text{Cu}_2(\mu\text{-dppm})_2\text{L}_A]^{2+}$ with the hydrogen atoms omitted and only the *ipso* carbons of the phenyl rings shown. Ellipsoids are drawn at the 50% probability level. (b) The boat-chair conformation of the $[\text{Cu}(\mu\text{-dppm})_2]$ ring.

angles range from 1.47° to 4.81°). Together they form an eight-membered $\text{Cu}(\mu\text{-dppm})_2\text{Cu}$ ring in a boat-chair conformation (see Fig. 1b). A similar feature has been observed in other compounds such as $[\text{Cu}_2(\mu\text{-dppm})_2(\mu\text{-PPDMe})]^{2+}$ (PPDMe 3,6-bis(3,5-dimethylpyrazol-1-yl)pyridazine).²³

In each complex, the copper atoms have a distorted tetrahedral arrangement determined by two phosphorus atoms (of two *dppm* ligands) and two nitrogen atoms (one from the pyridazine, one from a pyridine of **L**). The N–Cu–N angles are acute [range $76.0(1)^\circ$ – $77.7(3)^\circ$] due to the small chelating bite angle typical of *bppn* ligands.²⁴ The P–Cu–P units are non-linear [range $124.21(5)^\circ$ – $130.57(5)^\circ$], resulting in a folding of the Cu_2P_4 core along the Cu···Cu axis in an analogous disposition to that of the starting material $[\text{Cu}(\mu\text{-dppm})(\text{NO}_3)]_2$.²⁵

The Cu–P and Cu–N bond lengths (see Table 1) are in the typical range of four coordinate copper(I) complexes. More notable is that the bis-(2-pyridyl)pyridazine fragment of the ligand **L** is not completely planar, as is shown by the dihedral angles of the pyridine rings with respect to the pyridazine one (torsion angles $[\text{Cu}_2(\mu\text{-dppm})_2(\mu\text{-L})](\text{NO}_3)_2$ **L**_A 29.86° , 23.09° ; **L**_B 29.60° , 22.53°). Also the aryl substituents are twisted significantly out-of-the-plane of the pyridazine ring, almost to perpendicular (torsion angles $[\text{Cu}_2(\mu\text{-dppm})_2(\mu\text{-L})](\text{NO}_3)_2$ **L**_A 70.71° , 78.00° ; **L**_B 72.86° , 77.37°). Ring twisting is necessary to relieve steric

congestion, and is achieved by the rotation of both arene rings.

Both structures exhibit weak intramolecular $\pi \cdots \pi$ interactions (range **L**_A 3.42 – 3.72 Å, **L**_B 3.43 – 3.76 Å) between the phenyl rings on the same *dppm* ligand and between the phenyl rings of the *dppm* and both 2-pyridine rings of the *bppn* **L** (see Fig. S2†). These interactions play an important role in stabilising the structure and probably contribute to the optical properties observed in the solid state.

The presence of these binuclear structures in solution is confirmed by ^1H NMR spectroscopy (CDCl_3 , room temperature). The methylene protons of the *dppm* (CH_2P_2) resonate as two unresolved multiplets. These relate to the (ABX_2) spin system of the two sets of chemically inequivalent protons $\text{CH}_2\text{H}_2\text{P}$ ($[\text{Cu}_2(\mu\text{-dppm})_2(\mu\text{-L})]^{2+}$: **L**_A δ 3.94, 3.51 ppm; **L**_B δ 3.99, 3.55 ppm; **L**_C δ 3.98, 3.60 ppm) and are typical of binuclear complexes containing an eight-membered “ $\text{Cu}_2(\mu\text{-dppm})_2$ ” moiety.²³ The aromatic protons of the *dppm* ligands appear as two different sets of signals (see the NMR spectra for $[\text{Cu}_2(\mu\text{-dppm})_2(\mu\text{-L}_C)]^{2+}$ in Fig. S3 and S4†) due to the different positions (equatorial and axial positions) of the phenyl rings in the eight-membered cycle (see Fig. 1b). The resonances of the two coordinated pyridine rings of the *bppn* ligands **L** are chemically equivalent consistent with the proposed symmetrical dichelate bridging system of **L** and in agreement with the solid-state molecular structure.

Room temperature $^{31}\text{P}\{^1\text{H}\}$ NMR spectra exhibit a single resonance as expected for the phosphorus atoms in each molecule ($[\text{Cu}_2(\mu\text{-dppm})_2(\mu\text{-L})]^{2+}$: **L**_A δ -8.11 ppm, **L**_B δ -6.50 ppm, **L**_C δ -6.35 ppm). These resonances are shifted to a lower field compared to the free ligand (-21.32 ppm) in a region similar to that of the precursor complex $[\text{Cu}(\mu\text{-dppm})(\text{NO}_3)]_2$ ($^{31}\text{P}\{^1\text{H}\}$ -9.31 ppm).²⁵

ESI mass spectra gave parent peaks corresponding to m/z $[\text{Cu}_2(\text{dppm})_2\text{L}]^{2+}$, which matched the simulated isotopic distribution patterns and confirmed the formation of the dinuclear dications.

Photophysical and electrochemical properties

The absorption spectra of the ligands *bppn* **L** and of the complexes $[\text{Cu}_2(\mu\text{-dppm})_2(\mu\text{-L})]^{2+}$ were obtained in CH_2Cl_2 and the results are shown in Table 2. The spectra of the free ligands **L**_A and **L**_B are similar, with two absorption bands λ_{max} 266–268 and 325–329 nm, attributed to the transitions centred on the bispyridylpyridazine. In the case of **L**_C, there is a lower energy band (370 nm) due to the fluoranthene. The absorption spectra of the complexes are similar to those of the ligands but in addition they have a weak, broad, low-energy shoulder in the λ 370–425 nm region (Table 2), which is responsible for the orange colour of the complexes (Fig. 2). This low-energy band is attributed to MLCT transitions involving the *N,N*-chelate ligand and the Cu(I) ion (perhaps influenced by the phosphine ligand).^{26,27} In agreement with this MLCT assignment, the low-energy absorption of the $[\text{Cu}_2(\mu\text{-dppm})_2(\mu\text{-L}_C)]^{2+}$ complex is slightly red shifted compared to the others, as the diazafluoranthene-containing ligand stabilizes the π^* orbitals (Fig. 2).

Electrochemical studies of the ligands showed no oxidation processes in the potential ranges (0 V–2 V vs. SCE). The ligand reduction of the three complexes and the reductions of the free ligands were reversible and lowered upon complexation (see Table 2). This is consistent with σ -bonding of the ligand to the metal

Table 2 Absorption (dichloromethane, 5×10^{-5} M) and electrochemical [acetonitrile (or dimethylformamide in the case of L_C due to its poor solubility), 1×10^{-3} M] data for L_A , L_B , L_C and the corresponding copper complexes. Electrochemical measurements were recorded at room temperature, using a glassy carbon working electrode, a Pt wire counter electrode and a SCE reference electrode, using a scan rate of 100 mV/s. Potentials are quoted vs. Fc/Fc⁺, which was used as an internal standard

	λ/nm ($\epsilon/10^3 \text{ M}^{-1}\text{cm}^{-1}$)	$E_{1/2}^{\text{ox}}/\text{V}$	$E_{1/2}^{\text{red}}/\text{V}$
L_A	266 (16.9), 325 (1.2)	—	-1.22, -1.94 ^a , -2.32 ^b
L_B	268 (26.9), 329 (0.9)	—	-1.22 ^a , -2.01 ^a
L_C	271 (28.2), 308 (17.8), 326 (13.2), 370 (13.4)	—	-1.24, -2.01
$[\text{Cu}_2(\mu\text{-dppm})_2L_A]^{2+}$	260 (71.6), 328 (21.6), 380 (10.2)	1.17 ^b	-1.34, -1.87
$[\text{Cu}_2(\mu\text{-dppm})_2L_B]^{2+}$	274 (76.7), 331 (21.2), 373 (11.7)	1.07 ^b	-1.33, -1.71 ^b , -1.93, -2.14 ^a
$[\text{Cu}_2(\mu\text{-dppm})_2L_C]^{2+}$	275 (72.5), 326 (36.0), 374 (32.8), 426 (16.1)	1.15 ^b	-1.14, -1.67, -1.97

^a quasi-reversible; ^b irreversible process, peak potentials quoted.

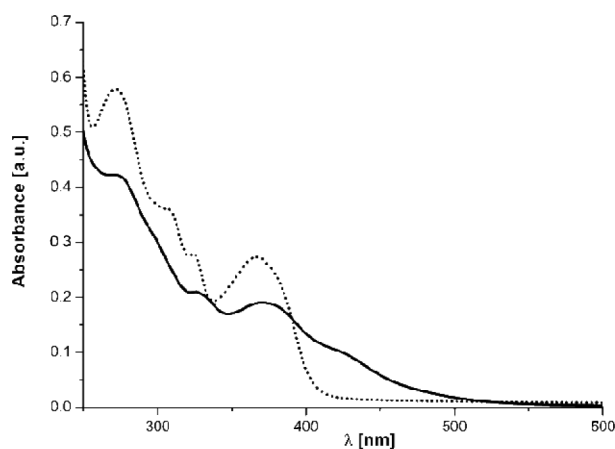


Fig. 2 The UV-vis spectra in dichloromethane of L_C (broken line) and $[\text{Cu}_2(\mu\text{-dppm})_2L_C]^{2+}$ (solid line) where the MLCT is clearly observed.

centre and the positive charge of the metal complex, which render the ligands more electron-accepting on complexation. The first reduction potential for $[\text{Cu}_2(\mu\text{-dppm})_2L_C]^{2+}$ reflects the greater electron-accepting nature of the aromatic platform in L_C , but subsequent reductions appear to be affected by the pyridyl or phenyl substituents. A broad irreversible oxidation band was observed for each complex that was assigned to the Cu(I)/Cu(II) redox couple on comparison with similar data reported in the literature (see Fig. S5† and Table 2).^{28–30} Such oxidations occur at high potentials because of the need to radically alter the complex geometry for Cu(II) and are indicative of ligand rigidity. The irreversible character of the oxidation process in all cases

indicates that the Cu(II) species rapidly decompose on forming, as revealed by the disappearance of the oxidation peak under repetitive scans (Fig. S5†). The intensity and the broad character of the oxidations imply that multiple electron-transfer is occurring, which must originate from the presence of two metal centres. ¹H NMR investigations of the electrochemically oxidised solutions did not shed any light on the identity of the decomposition products.

All the ligands and their respective copper complexes were weakly luminescent in the solid state, in solution at room temperature and in frozen solution at 77 K. Photoluminescence spectra and lifetime data are summarised in Table 3 (complexes) and Table S1† (ligands). For the copper systems, all the spectra are broad without vibronic progression, suggesting that the emissive excited states have charge transfer character. In solid state, the ligands *bppn* L present high energy emissions (~350–490 nm) with excited state lifetimes in the nanosecond range. In the case of L_C , a lower energy band is also observed (~600 nm). Considering the longer lifetime of this band, this emission could have some triplet state character (e.g. from a ³ $\pi\pi^*$ excited state localised on the π -conjugated fluoranthene chromophore), or could be intra-ligand charge transfer in nature (Table S1†).

In the solid state at room temperature, the compounds exhibit a red-orange luminescence (see Fig. 3), with the bands detected in the range between λ 587 and 676 nm ascribable to radiative decay from the MLCT states.^{1,31} In the case of $[\text{Cu}_2(\mu\text{-dppm})_2(\mu\text{-}L_A)]^{2+}$ (λ_{em} 635 nm) and $[\text{Cu}_2(\mu\text{-dppm})_2(\mu\text{-}L_B)]^{2+}$ (λ_{em} 642 nm), the emissions are similar, but for $[\text{Cu}_2(\mu\text{-dppm})_2(\mu\text{-}L_C)]^{2+}$ (λ_{em} 676 nm), the emission is red shifted due to the presence of the diazafluoranthene, which increases the degree of π -conjugation

Table 3 Comparative Photophysical data of complexes ($[\text{Cu}_2(\mu\text{-dppm})_2(\mu\text{-}L)]^{2+}$)

		T/K	λ_{em} [nm]	ϕ	$\tau/\mu\text{s}$
$[\text{Cu}_2(\mu\text{-dppm})_2(\mu\text{-}L_A)]^{2+}$	solid	298	587 <i>sh</i> , 635, 660 <i>sh</i> (λ_{exc} 500)	0.013	1.0 (100%) (λ_{exc} 460 – λ_{em} 630)
		77	670 (λ_{exc} 495)		5.2 (74%), 0.7 (26%) (λ_{exc} 460 – λ_{em} 670)
	CH_2Cl_2	298	670 <i>br</i> (λ_{exc} 400)		1.1 (89%), 1.3 (11%) (λ_{exc} 460 – λ_{em} 630)
$[\text{Cu}_2(\mu\text{-dppm})_2(\mu\text{-}L_B)]^{2+}$	solid	298	643, 664 _{max} (λ_{exc} 500)	0.009	0.3 (100%) (λ_{exc} 460 – λ_{em} 640)
		77	642, 666 <i>sh</i> (λ_{exc} 490)		4.6 (73%), 0.6 (27%) (λ_{exc} 460 – λ_{em} 680)
	CH_2Cl_2	298	681 (λ_{exc} 500)		2.3 (87%), 0.1 (13%) (λ_{exc} 460 – λ_{em} 675)
$[\text{Cu}_2(\mu\text{-dppm})_2(\mu\text{-}L_C)]^{2+}$	solid	298	675 <i>br</i> (λ_{exc} 450)	0.021	0.6 (100%) (λ_{exc} 460 – λ_{em} 675)
		77	678 (λ_{exc} 450)		4.7 (72%), 0.7 (28%) (λ_{exc} 460 – λ_{em} 695)
	CH_2Cl_2	298	676 (λ_{exc} 550)		22.8 (85%), 1.0 (15%) (λ_{exc} 460 – λ_{em} 670)
		77	645 <i>sh</i> , 695 (λ_{exc} 495)		
		77	675 _{max} <i>br</i> (λ_{exc} 450)		
		77	685 (λ_{exc} 450)		

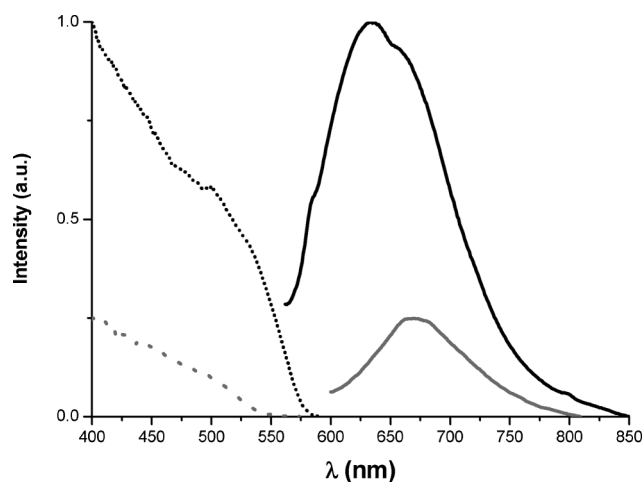


Fig. 3 Excitation (broken line) and emission (solid line) spectra of $[\text{Cu}_2(\mu\text{-dppm})_2(\mu\text{-L}_A)](\text{NO}_3)_2$ in solid state at room temperature (black) and at 77 K (grey).

and thus stabilizes the π^* of the ligand, with concurrent consequences for $^3\text{MLCT}$ emissive states. These red-orange emissions for heteroleptic copper compounds are quite unusual (bipyridine and phenanthroline complexes usually emit in the green region) and only a few examples have been found in the literature.^{16,32} They could be related to the dinuclear nature of these systems.

When cooling the solid samples ($T = 77$ K), the emissions undergo a small red-shift and are less intense ($[\text{Cu}_2(\mu\text{-dppm})_2(\mu\text{-L}_A)]^{2+}$ 298 K λ_{em} 635 nm, 77 K λ_{em} 670 nm; $[\text{Cu}_2(\mu\text{-dppm})_2(\mu\text{-L}_B)]^{2+}$ 298 K λ_{em} 642 nm, 77 K λ_{em} 681 nm; $[\text{Cu}_2(\mu\text{-dppm})_2(\mu\text{-L}_C)]^{2+}$ 298 K λ_{em} 676 nm, 77 K λ_{em} 695 nm). As proposed by McMillin, this relatively unusual phenomenon may be attributed to the presence of a thermal equilibrium between two emissive states, $^1\text{MLCT}$ and $^3\text{MLCT}$, where $^3\text{MLCT}$ dominates at low temperature, shifting the emission maximum to lower energy (see Fig. 3).¹ For CH_2Cl_2 solutions, the luminescence is quenched almost completely. However, when the samples are thoroughly purged with oxygen through several freeze-thaw-pump cycles under low pressure, a weak red-orange emission is observed in all the complexes (see Fig. 4), which is slightly red-shifted with respect to the solid state for $[\text{Cu}_2(\mu\text{-dppm})_2(\mu\text{-L})]^{2+}$ ($\text{L} = \text{L}_A, \text{L}_B$) ($[\text{Cu}_2(\mu\text{-dppm})_2(\mu\text{-L}_A)]^{2+}$ solid λ_{em} 635 nm, CH_2Cl_2 λ_{em} 670 nm; $[\text{Cu}_2(\mu\text{-dppm})_2(\mu\text{-L}_B)]^{2+}$ solid λ_{em} 642 nm, CH_2Cl_2 λ_{em} 675 nm). No changes within the concentration (range 10^{-5} M– 10^{-3} M) were observed. The solution emission quantum yields determined according to the method described by Demas³³ (Table 2) are poor and in the range 0.009 to 0.021, similar to those observed for analogous copper complexes.^{31,34–36}

The complexes show long lifetimes in the microsecond range in the solid state and in solution at room temperature. In solid state at room temperature these systems present a monoexponential decay, however, in solution and in solid state at low temperature, the decay has two components, best modelled by a biexponential function. Although biexponential decay is unusual for copper complexes it is not without precedence.^{37,38} The excited state lifetimes of the ligands (Table S1†) exhibit similar exponential-type behaviour. For $[\text{Cu}_2(\mu\text{-dppm})_2(\mu\text{-L})]^{2+}$ ($\text{L} = \text{L}_A, \text{L}_B$), the lifetimes are very similar and in both cases longer in solution than in the solid state ($[\text{Cu}_2(\mu\text{-dppm})_2(\mu\text{-L}_A)]^{2+}$ solid 1.0 μs , CH_2Cl_2 1.1 μs ; $[\text{Cu}_2(\mu\text{-dppm})_2(\mu\text{-L}_B)]^{2+}$ solid 0.3 μs , CH_2Cl_2 2.3 μs).

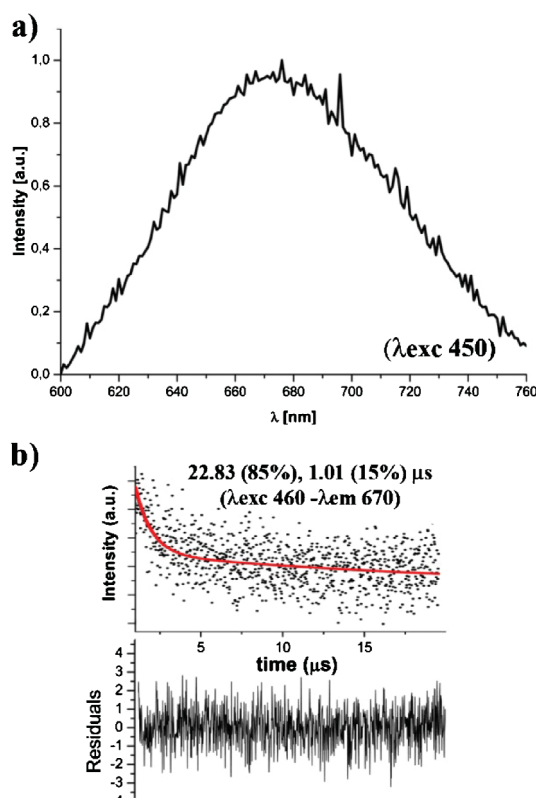


Fig. 4 Normalized emission spectrum of $[\text{Cu}_2(\mu\text{-dppm})_2(\mu\text{-L}_C)](\text{NO}_3)_2$ in degassed dichloromethane solution at room temperature (a) and its emission decay with fitting (b).

The presence of the weak $\pi \cdots \pi$ interactions observed in crystalline samples could increase the non-radiative relaxation paths and thus explain the shorter lifetimes in the solid state. The excited state lifetime of $[\text{Cu}_2(\mu\text{-dppm})_2(\mu\text{-L}_C)]^{2+}$ as a solid is shorter than that observed for the others (0.6 μs), here $\pi \cdots \pi$ interactions involving the fluoranthene moieties would be expected to be stronger than those observed for $[\text{Cu}_2(\mu\text{-dppm})_2(\mu\text{-L})]^{2+}$ ($\text{L} = \text{L}_A, \text{L}_B$) and could contribute to the deactivation of the excited state. However, in oxygen-free solution, this complex $[\text{Cu}_2(\mu\text{-dppm})_2(\mu\text{-L}_C)]^{2+}$ has a longer lifetime of 22.8 μs . As far as we know, this value is the longest found for a system of the type $[\text{Cu}(\text{N}^{\wedge}\text{N})(\text{P}^{\wedge}\text{P})]^+$, being longer than that previously described by Armaroli for $[\text{Cu}(\text{POP})(\text{dmdp-phen})]^+$ (2,9-dimethyl-4,7-diphenylphenanthroline) under the same conditions (17.3 μs in dichloromethane at room temperature).¹² It should be noted however that the neutral amidophosphine complexes of copper $[\text{RPN}]\text{Cu}(\text{L})_2$ reported by Miller and co-workers in some cases present longer lifetimes (16–150 μs).³⁹ Although neutral complexes are highly desirable, some examples of OLED devices with charged species as active materials have been reported.⁴⁰ In all cases the consideration of emission lifetimes is important; guest phosphors ideally exhibit a phosphorescence lifetime in the region of 5–50 μs at room temperature.⁴¹ The desirable solid-state photophysics of the simple systems reported here can be attributed to the rigid conformation of the eight-membered ring, which precludes the possible distortion of the copper in the excited state and the formation of quenching exciplexes.

Conclusions

The use of extended polyaromatic pyridazines and aza fluoranthenes as new N-donor ligand motifs in the formation of dimeric Cu(I) bisphosphine complexes has resulted in three novel sterically hindered dication systems. The N-donor ligands act as bridging supports to a rigid eight-membered ring comprising $\text{Cu}(\mu\text{-dppm})_2\text{Cu}$ and provide a stable framework to secure the distorted tetrahedral geometry of the Cu centres. Red-orange MLCT emission is characteristic of these complexes and the structural features give rise to emission lifetimes in the microsecond range similar to those associated with neutral amidophosphine complexes.

Experimental

General Methods

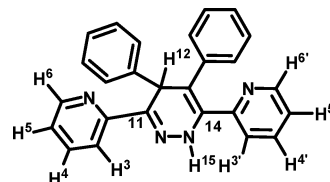
Elemental analyses were carried out in a Perkin–Elmer 240-B analyser. NMR spectra were recorded on a DPX-400 spectrometer by using the standard references. Electrospray ionization mass spectra were recorded on a micromass LCT electrospray mass spectrometer. Nuclear magnetic resonance spectra were recorded with a Bruker Avance DPX-400 MHz at the following frequencies: 400.1 MHz for ^1H , 100.6 MHz for $^{13}\text{C}\{^1\text{H}\}$ and 162.2 for $^{31}\text{P}\{^1\text{H}\}$. Chemical shifts are reported in ppm relative to external standards (SiMe_4 for ^1H and $^{13}\text{C}\{^1\text{H}\}$ and 85% H_3PO_4 for $^{31}\text{P}\{^1\text{H}\}$) and all the coupling constants are given in Hz to two decimal places.

UV-vis spectra were obtained on a Shimadzu UV-2401PC UV-vis spectrometer. Emission and excitation spectra were obtained on a Fluorolog FL-3-11 spectrofluorimeter. A Jobin Yvon FluoroHub single photon counting controller fitted with an appropriate wavelength Jobin Yvon NanoLED was used to measure lifetimes, which were determined from the observed decays using DataStation v2.4. The solution emission quantum yields were measured by the Demas and Crosby method using $[\text{Ru}(\text{bipy})_3]\text{Cl}_2$ in degassed water as standard ($\phi_{450\text{nm}} 0.042$).³³ All electrochemical experiments were performed with a CH Instrument Potentiostat, model 660B. Cyclic voltammograms were measured on 1 mM solutions of the complexes in dry, degassed acetonitrile or dimethylformamide with tetrabutylammonium hexafluorophosphate (TBAPF_6 , 0.1 M) as the supporting electrolyte with a glassy carbon working electrode, a Pt wire counter electrode and a saturated calomel electrode as the reference electrode. All the potentials were referenced to internal ferrocene added at the end of each experiment.

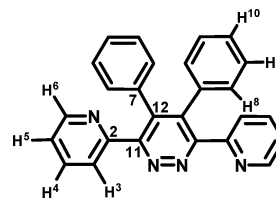
3,6-bis(2-pyridyl)-1,2,4,5-tetrazine (bptz),¹⁹ 3,6 bis(2-pyridyl)-8,9-diazafluoranthene (L_c)²⁰ and $[\text{Cu}(\mu\text{-dppm})(\text{NO}_3)_2]$ ²⁵ were prepared by literature methods. *Trans*-stilbene and 1,4-di(4-pyridyl)ethylene were purchased from Aldrich.

Synthesis of 3,6-bis(2-pyridyl)-4,5-diphenyl hydroypyridazine. 3,4-bis(2-pyridyl)-1,2,4,5-tetrazine (0.600 g, 2.540 mmol) and *trans*-stilbene (0.469 g, 2.600 mmol) were refluxed in 20 mL of toluene for 24 h. At this stage, the colour of the solution had changed from dark pink to bright yellow. The solvent was removed under vacuum, and the reaction mixture was purified by running it through a column of silica (10% diethyl ether in dichloromethane) obtaining as a pure yellow solid (0.906 g, 92%). Anal. calcd for $\text{C}_{26}\text{H}_{20}\text{N}_4$ (388.47): C 80.39, H 5.19, N 14.42. Found: C 79.99, H

5.56, N 14.49. δ_{H} (400 MHz; CDCl_3 ; Me_4Si) 9.43 (s, 1H, H^{15}), 8.67 (d, 1H, H^6 , $J = 3.8$ Hz), 8.61 (d, 1H, H^6 , $J = 4.4$ Hz), 8.10 (d, 1H, H^7 , $J = 7.9$ Hz), 7.63 (Ψtd , 1H, H^4 , $J = 7.8, 1.8$ Hz), 7.57 (d, 2H, H^8 , $J_{\text{g},\text{r}} = 7.0$ Hz), 7.40 (Ψtd , 1H, H^4 , $J = 7.8, 1.5$ Hz), 7.30–7.17 (m, 11H, H^{Ph}), 5.82 ppm (s, 1H, H^{12}). δ_{C} (101 MHz; CDCl_3 ; Me_4Si) 154.18 (1C, C11), 151.56 (1C C14), 149.02 (1C C6), 148.30 (1C C6'), 141.85 (1C CQ), 138.85 (1C CQ), 136.08 (1C C4'), 135.86 (1C C4'), 135.11 (1C CQ), 129.85 (1C), 128.54 (1C C3), 128.27 (1C C5), 128.25 (1C), 127.16 (1C), 126.70 (1C), 125.47 (1C), 123.02 (1C), 122.67 (1C), 121.48 (1C), 108.15 (1C C13), 41.54 ppm (1C C12). HRMS (CH_3CN); calculated $[\text{MH}]^+ m/z$ 389.1766, found: 389.1782⁺.



Synthesis of 3,6-bis(2-pyridyl)-4,5-diphenyl pyridazine (L_A). 20 mL of a 6 M solution of NaNO_2 was added dropwise to a solution of concentrated HCl (12 mL). The gas formed was then passed through a 40 mL dichloromethane solution containing 0.807 g (2.093 mmol) of 3,6-bis(2-pyridyl)-4,5-diphenyl hydroypyridazine, by blowing nitrogen through the acid and into the dichloromethane solution. When all the sodium nitrite had been added, the dichloromethane solution was allowed to return to room temperature. The solvent was evaporated and the reaction mixture dissolved in water and neutralized with the addition of 10% ammonia solution. The mixture was extracted into CH_2Cl_2 , dried over MgSO_4 and run through a column of silica (10% methanol in ethyl acetate) recovering a white product L_A (0.598 g, 74%). Anal. calcd for $\text{C}_{26}\text{H}_{18}\text{N}_4$ (386.46) C 80.81, H 4.69, N 14.50. Found: C 80.92, H 4.64, N 14.26. δ_{H} (400 MHz; CD_3CN ; Me_4Si) 8.42 (d, 2H, H^6 , $J = 4.5$ Hz), 7.64 (m, 4H, $\text{H}^{3,4}$), 7.17 (Ψtd , 2H, H^5 , $J = 6.5, 1.5$ Hz), 7.05 (m, 6H, H^8 , H^{10}), 6.87 ppm (m, 2H, H^9). δ_{C} (101 MHz; CDCl_3 ; Me_4Si) 158.50 (2C, C11), 155.55 (2C, C2), 148.42 (2C, C6), 138.72 (2C, C12), 135.72 (2C, C4), 134.20 (2C, C7), 129.67 (4C, C8), 127.11 (4C, C9), 126.86 (2C, C10), 124.58 (2C, C3), 122.48 ppm (2C, C5). HRMS (CH_3CN); calculated $[\text{MH}]^+ m/z$ 387.1596, found: 387.1610

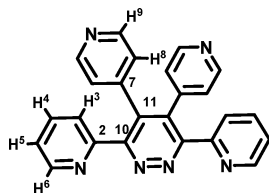


Synthesis of 3,6-bis(2-pyridyl)-4,5-bis(4-pyridyl)-hydroypyridazine. This compound was prepared as a bright yellow solid (0.618 g, 75%) similarly to compound L_A starting from 3,4-bis(2-pyridyl)-1,2,4,5-tetrazine (0.500 g, 2.116 mmol) and 1,4-bis(4-pyridyl)-ethylene (0.410 g, 2.251 mmol) and purified by column chromatography on silica (20% methanol in diethyl ether). Anal. calcd for $\text{C}_{24}\text{H}_{18}\text{N}_6$ (390.45) C 79.54, H 5.01, N 15.46. Found: C 80.01, H 5.11, N 15.72. δ_{H} (400 MHz; CD_3CN ; Me_4Si) 9.50 (s, 1H, H^{16}), 8.72 (d, 1H, H^6 , $J = 5.0$ Hz), 8.61 (d, 1H, H^6 , $J = 6.0$ Hz), 8.50 (d, 2H, $\text{H}^{9/9'}$, $J = 6.5$ Hz), 8.41 (d, 2H, $\text{H}^{9/9'}$, $J = 6.0$ Hz), 8.13 (d, 1H, H^7 , $J = 8.0$ Hz), 7.66 (Ψtd , 1H, H^4 , $J = 7.8, 1.5$ Hz), 7.55

(Ψ td, 1H, H⁴, J = 7.5, 1.5 Hz), 7.46 (d, 2H, H^{8/8'}, J = 6.0 Hz), 7.36 (d, 1H, H³, J = 6.0 Hz), 7.32 (d, 1H, H⁵, J = 2.0 Hz), 7.22 (m, 1H, H^{5'}, J = 2.0 Hz), 7.06 (d, 2H, H^{8/8'}, J = 6.0 Hz), 5.86 ppm (s, 1H, H¹²). δ_c (101 MHz; CDCl₃; Me₄Si) 153.39 (1C, C2'), 150.79 (1C, C2), 150.09 (1C, C9), 150.02 (1C, C9'), 150.00 (1C, C6), 148.42 (1C, C6'), 146.30 (1C, C7), 140.67 (1C, C10), 138.74 (2C, C13), 136.48 (2C, C4), 136.21 (1C, C4'), 125.64 (1C, C3), 124.14 (1C, C5), 123.90 (1C, C8), 123.27 (1C, C5'), 123.09 (1C, C8'), 121.45 (1C, C3'), 102.52 (1C, C11), 39.48 (1C, C7'). HRMS (CH₃CN); calculated for C₂₄H₁₉N₆: [MH]⁺ m/z 391.1671, found: 391.1667.

Synthesis of 3,6-bis(2-pyridyl)-4,5-bis(4-pyridyl)-pyridazine (L_B).

This compound was prepared as an off-white product L_B (0.308 g, 50%) similarly to compound L_A, starting from NaNO₂ (20 mL, 6 M), HCl (12 mL) and 3,6-bis(2-pyridyl)-4,5-bis(4-pyridyl)-1,4-dihydropyridazine (0.618 g, 1.587 mmol). It was purified by column chromatography on silica (50% ether, 50% methanol). Anal. calcd for C₂₄H₁₆N₆ (388.43) C 74.21, H 4.15, N 21.64. Found: C 73.83, H 4.60, N 21.88. δ_H (400 MHz; CDCl₃; Me₄Si) 8.34 (d, 2H, H⁹, J = 5.5 Hz), 8.30 (d, 2H, H⁶, J = 4.5 Hz), 8.01 (d, 2H, H³, J = 7.6 Hz), 7.81 (Ψ td, 2H, H⁴, J = 7.5, 1.5 Hz), 7.23 (m, 2H, H⁵), 6.85 ppm (d, 2H, H⁸, J = 6.0 Hz). δ_c (101 MHz; CDCl₃; Me₄Si) 157.03 (4C, C10), 154.18 (2C, C2), 148.65 (4C, C9), 148.31 (2C, C6), 142.59 (2C, C7), 136.28 (2C, C4), 136.10 (2C, C11), 124.49 (2C, C3), 124.10 (2C, C8), 123.19 ppm (2C, C5). HRMS (CH₃CN); calculated: [MH]⁺ m/z 387.1504, found: 387.1515

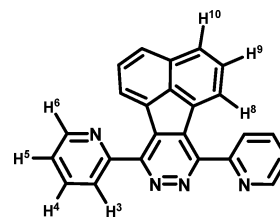


Synthesis of [Cu₂(μ -dppm)₂(μ -L_A)](NO₃)₂. 3,6-bis(2-pyridyl)-4,5-diphenyl pyridazine (L_A) (19 mg, 0.049 mmol) was added to a colourless solution of [Cu(μ -dppm)(NO₃)₂] (50 mg, 0.049 mmol) in DCM (10 mL) changing colour immediately to orange. The resulting mixture was stirred for 1 h, filtered through Celite and concentrated to 2 mL. The addition of Et₂O (20 mL) affords the precipitation of [Cu₂(μ -dppm)₂(μ -L_A)](NO₃)₂ as an orange solid (62 mg, 90%), which was filtered, washed with cold MeOH and dried. Anal. calcd for C₇₆H₆₂N₆Cu₂P₄O₆·1.5 CH₂Cl₂ (1533.74) C 60.68, H 4.69, N 5.48. Found C 60.17, H 4.14, N 5.49. δ_H (400 MHz; CDCl₃; Me₄Si) 8.09 (2H, d, J = 3.6, H6), 7.60 (4H, d, J = 6.0, H8), 7.43 (18H, m br, H3, H4, H9, H10 and Ho), 7.29 (4H, t, J = 6.0, Hp), 7.22 (8H, t, J = 6.8, Hm, dppm), 7.00 (2H, t, J = 6.1, H5), 6.93 (4H, t, J = 7.5, Hp'), 6.81 (16H, m br, Ho' and Hm'), 3.94 (2H, m br, P-CH₂-P), 3.51 ppm (2H, m br, P-CH₂-P). δ_P (162 MHz; CDCl₃; 85% H₃PO₄) -8.11 ppm. δ_c (101 MHz; CDCl₃; Me₄Si) 152.95 (2C, C11), 149.34 (2C, C2), 148.79 (2C, C6), 143.93 (2C, C12), 137.02 (2C, C4), 133.32 (2C, C7), 132.28 (8C, br, Co), 131.33 (8C, br, Co'), 130.18 (4C, Cp), 129.68 (4C, C8), 129.40 (8C, Cp'), 129.14 (2C, C10), 128.75 (8C, Cm), 128.59 (4C, C9), 128.38 (2C, C3), 128.17 (8C, Cm'), 126.05 (2C, C5), 25.94 ppm (2C, br, PCH₂P) (Missing C_i). HRMS (CH₃CN); calculated: [Cu₂(μ -dppm)₂(L_A)]²⁺ m/z : 640.1259, found: 640.1237.

Synthesis of [Cu₂(μ -dppm)₂(μ -L_B)](NO₃)₂. This complex [Cu₂(μ -dppm)₂(μ -L_B)](NO₃)₂ was prepared as an orange solid

(67 mg, 97%) according to the general procedure given for [Cu₂(μ -dppm)₂(μ -L_A)](NO₃)₂ starting from 3,6-bis(2-pyridyl)-4,5-bis(4-pyridyl)pyridazine (L_B) (19 mg, 0.049 mmol) and [Cu(μ -dppm)(NO₃)₂] (50 mg, 0.049 mmol). Anal. calcd for C₇₄H₆₀N₈Cu₂P₄O₆·2CH₂Cl₂ (1578.18) C 57.84, H 4.09, N 7.10. Found C 57.37, H 3.89, N 7.00. δ_H (400 MHz; CDCl₃; Me₄Si) 8.70 (4H, s br, H9), 8.02 (2H, d, J = 4.2, H6), 7.76 (4H, d, J = 3.8, H8), 7.45 (10H, m br, H4 and Ho), 7.36 (2H, d, J = 8.3, H3), 7.19 (4H, t, J = 7.8, Hp), 7.19 (8H, t, J = 7.5, Hm), 7.10 (4H, t, J = 7.1, Hp'), 6.90 (18H, m br, H5, Ho' and Hm'), 3.99 (2H, m br, P-CH₂-P), 3.55 (2H, m br, P-CH₂-P). δ_P (162 MHz; CDCl₃; 85% H₃PO₄) -6.50 ppm. δ_c (101 MHz; CDCl₃; Me₄Si) 151.94 (2C, C10), 150.61 (4C, C9), 149.37 (2C, C6), 148.38 (2C, C2), 132.87 (8C, br, Co), 132.47 (2C, C7), 131.54 (8C, br, Co'), 130.75 (4C, Cp), 130.19 (2C, C4), 129.69 (4C, Cp'), 129.03 (8C, Cm), 128.67 (8C, Cm'), 128.56 (2C, C11), 128.32 (2C, C3), 126.49 (2C, C5), 124.89 (4C, C8), 26.24 ppm (2C, br, PCH₂P) (Missing C_i). HRMS (CH₃CN); calculated: [Cu₂(μ -dppm)₂(L_B)]²⁺ m/z : 641.1211, found: 641.1202.

Synthesis of [Cu₂(μ -dppm)₂(μ -L_C)](NO₃)₂. This complex [Cu₂(μ -dppm)₂(μ -L_C)](NO₃)₂ (55 mg, 81%) was prepared as a deep orange solid similarly to [Cu₂(μ -dppm)₂(μ -L_A)](NO₃)₂ starting from 3,6-bis(2-pyridyl)-8,9-diazafluoranthene (L_C) (35 mg, 0.049 mmol) and [Cu(μ -dppm)(NO₃)₂] (50 mg, 0.049 mmol). The product was filtered, washed with cold MeOH and dried. Anal. calcd for C₇₄H₅₈N₆Cu₂P₄O₆·(1378.30) C 64.94, H 4.24, N 6.10. Found C 64.69, H 4.61, N 5.89. δ_H (400 MHz; CDCl₃; Me₄Si) 9.16 (2H, d, J = 8.0, H6), 8.87 (2H, d, J = 7.3, H8/H10), 8.87 (2H, d, J = 8.3, H8/H10), 8.34 (2H, d, J = 8.4, H3), 8.23 (2H, t, J = 7.8, H5), 8.08 (2H, d, J = 7.8, H9), 7.43 (12H, m br, Ho and Hp), 7.34 (2H, dd; J = 7.0, 5.0; H4), 7.29 (8H, t, J = 7.3, Hm), 6.89 (4H, t, J = 7.5, Hp'), 6.74 (8H, s br, Ho'), 6.62 (8H, t, J = 7.5, Hm'), 3.98 (2H, m br, P-CH₂-P), 3.60 ppm (2H, m br, P-CH₂-P). δ_P (162 MHz; CDCl₃; 85% H₃PO₄) -6.35 ppm. ¹³C{¹H} not obtained due to poor solubility. HRMS (CH₃CN); calculated: [Cu₂(μ -dppm)₂(L_C)]²⁺ m/z : 626.1102, found: 626.1081.



Acknowledgements

We wish to acknowledge the technical contribution of Dr John O'Brien, Dr Manuel Ruether and Dr Martin Feeney. We acknowledge the funding provided by Science Foundation Ireland-SFI-08RFPCH1465 (DN), 05PICA1819 (GC, SV, GOM) and EU-FP6-MTKD014472 (BG, LW).

References

- 1 N. Armaroli, G. Accorsi, F. Cardinali and A. Listorti, *Top. Curr. Chem.*, 2007, **280**, 69–115.
- 2 N. Armaroli, *Chem. Soc. Rev.*, 2001, **30**, 113–124.

- 3 A. Lavie-Cambot, M. Cantuel, Y. Leydet, G. Jonusauskas, D. M. Bassani and N. D. McClenaghan, *Coord. Chem. Rev.*, 2008, **252**, 2572–2584.
- 4 S. Campagna, F. Puntoriero, F. Nastasi, G. Bergamini and V. Balzani, *Top. Curr. Chem.*, 2007, **280**, 117–214.
- 5 J. A. G. Williams, *Top. Curr. Chem.*, 2007, **281**, 205–268.
- 6 L. Flamigni, A. Barbieri, C. Sabatini, B. Ventura and F. Barigelletti, *Top. Curr. Chem.*, 2007, **281**, 143–203.
- 7 G. Cooke, G. M. Ó Máille, R. Quesada, L. Wang, S. Varughese and S. M. Draper, *Dalton Trans.*, 2011, DOI: 10.1039/c1dt10340g.
- 8 D. J. Gregg, C. M. A. Ollagnier, C. M. Fitchett and S. M. Draper, *Chem.–Eur. J.*, 2006, **12**, 3043–3052.
- 9 D. J. Gregg, E. Bothe, P. Höfer, P. Passaniti and S. M. Draper, *Inorg. Chem.*, 2005, **44**, 5654–5660.
- 10 S. Varughese, G. Cooke and S. M. Draper, *Cryst. Eng. Comm.*, 2009, **11**, 1505–1508.
- 11 M. T. Buckner and D. R. McMillin, *J. Chem. Soc., Chem. Commun.*, 1978, 759–761.
- 12 N. Armaroli, G. Accorsi, M. Holler, O. Moudam, J.-F. Nierengarten, Z. Zhou, R. T. Wegh and R. Welter, *Adv. Mater.*, 2006, **18**, 1313–1136.
- 13 E. J. Fernandez, A. Laguna, J. M. Lopez-de-Luzuriaga, M. Monge, M. Montiel, M. E. Olmos and M. Rodriguez-Castillo, *Dalton Trans.*, 2009, 7509–7518.
- 14 C. Vogler, H.-D. Hausen, W. Kaim, S. Kohlmunn, H. E. A. Krumer and J. Rieker, *Angew. Chem., Int. Ed. Engl.*, 1989, **28**, 1659–1660.
- 15 W. L. Jia, T. McCormick, Ye Tao, J.-P. Lu and S. Wang, *Inorg. Chem.*, 2005, **44**, 5706–5712.
- 16 T. Tsubomura, S. Enoto, S. Endo, T. Tamane, K. Matsumoto and T. Tsukuda, *Inorg. Chem.*, 2005, **44**, 6373–6378.
- 17 H. Sleiman, P. N. W. Baxter, J.-M. Lehn, K. Airola and K. Rissanen, *Inorg. Chem.*, 1997, **36**, 4734–4742.
- 18 B. L. Schottel, H. T. Chifotides, M. Shatruk, A. Chouai, L. M. Pérez, J. Bacsá and K. R. Dunbar, *J. Am. Chem. Soc.*, 2006, **128**, 5895–5912.
- 19 D. L. Borger, *Chem. Rev.*, 1961, **86**, 781–793.
- 20 T. Sasaki, K. Kanematsu and T. Hiramatsu, *J. Chem. Soc., Perkin Trans. 1*, 1974, 1213–1215.
- 21 E. C. Constable, C. E. Housecroft, M. Neuburger, S. Reymann and S. Schaffner, *Eur. J. Org. Chem.*, 2008, 1597–1607.
- 22 A. Bondi, *J. Phys. Chem.*, 1964, **68**, 441–451.
- 23 J. Diez, P. Gamasa, J. Gimeno, M. Lanfranchi and A. Tiripicchio, *J. Chem. Soc., Dalton Trans.*, 1990, 1027–1033.
- 24 W. Kaim, *Coord. Chem. Rev.*, 2002, **230**, 127–139.
- 25 R. Yang, K. Lin, Y. Hou, D. Wang, D. Jin, B. Luo and L. Chen, *Transition Met. Chem.*, 1997, **22**, 254–258.
- 26 L. Yang, J.-K. Feng, A.-M. Ren, M. Zhang, Y.-G. Ma and X.-D. Liu, *Eur. J. Inorg. Chem.*, 2005, 1867–1879.
- 27 Y.-Q. Wei, K.-C. Wu, B.-T. Zhuang and Z.-F. Zhou, *J. Coord. Chem.*, 2006, **59**, 713–719.
- 28 A. Listorti, G. Accorsi, Y. Rio, N. Armaroli, O. Moudam, A. Gégout, B. Delavaux-Nicot, M. Holler and J.-F. Nierengarten, *Inorg. Chem.*, 2008, **47**, 6254–6261.
- 29 S.-B. Zhao, R.-Y. Wang and S. Wang, *Inorg. Chem.*, 2006, **45**, 5830–5840.
- 30 S.-M. Kuang, D. G. Cuttall, D. R. McMillin, P. E. Fanwick and R. A. Walton, *Inorg. Chem.*, 2002, **41**, 3313–3322.
- 31 Q. Zhang, Q. Zhou, Y. Cheng, L. Wang, D. Ma, X. Jing and F. Wang, *Adv. Funct. Mater.*, 2006, **16**, 1203–1208.
- 32 H. Araki, K. Tsuge, Y. Sasaki, S. Ishizaka and N. Kitamura, *Inorg. Chem.*, 2007, **46**, 10032–10034.
- 33 G. A. Crosby and J. N. Demas, *J. Phys. Chem.*, 1971, **75**, 991–1024.
- 34 Q. Zhang, Q. Zhou, Y. Cheng, L. Wang, D. Ma, X. Jing and F. Wang, *Adv. Mater.*, 2004, **16**, 432–436.
- 35 G. Che, Z. Su, W. Li, B. Chu, M. Li, Z. Hu and Z. Zhang, *Appl. Phys. Lett.*, 2006, **89**, 103511–103513.
- 36 A. Barbieri, G. Accorsi and N. Armaroli, *Chem. Commun.*, 2008, 2185–2193.
- 37 Z. Mao, H.-Y. Chao, Z. Hui, C.-M. Che, W.-F. Fu, K.-K. Cheung and N. Zhu, *Chem.–Eur. J.*, 2003, **9**, 2885–2897.
- 38 A. Tsuboyama, K. Kuge, M. Furugori, S. Okada, M. Hoshino and K. Ueno, *Inorg. Chem.*, 2007, **46**, 1992–2001.
- 39 A. J. M. Miller, J. L. Dempsey and J. C. Peters, *Inorg. Chem.*, 2007, **46**, 7244–7246.
- 40 Q. Zhang, Q. Zhou, Y. Cheng, L. Wang, D. Ma, X. Jing and F. Wang, *Adv. Mater.*, 2004, **16**, 432–436.
- 41 R. C. Evans, P. Douglas and C. J. Winscom, *Coord. Chem. Rev.*, 2006, **250**, 2093–2126.